Supplementary Information A: Thermal and Structural Stability of Platinum Nano-Accordion Structures

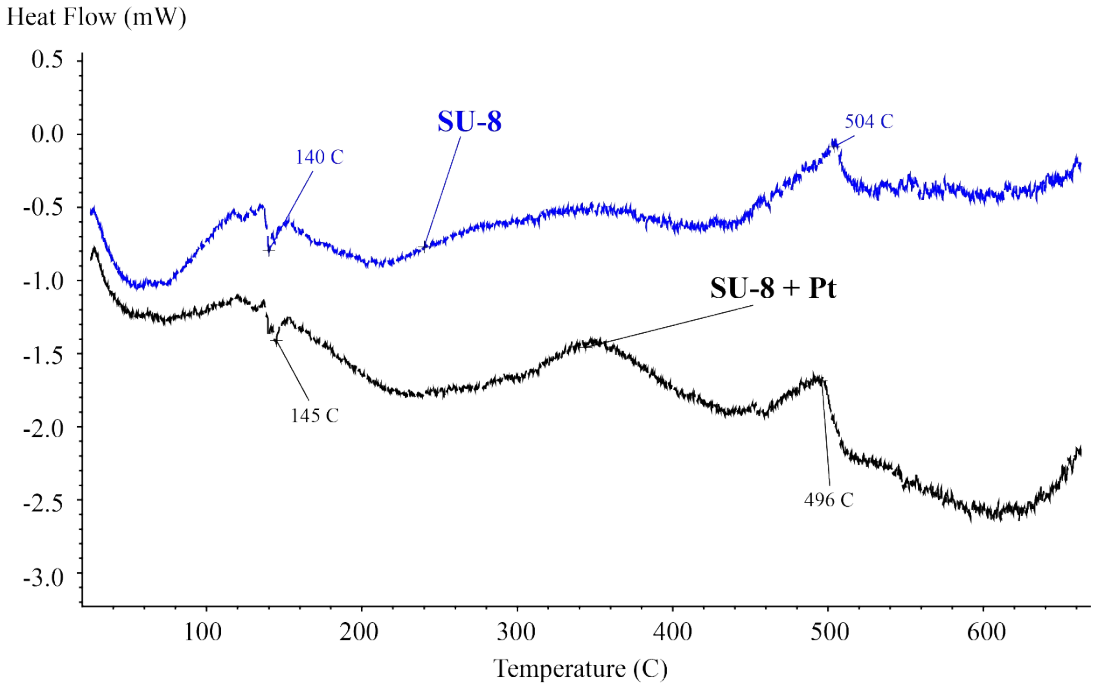

Figure S1. Differential scanning calorimetry (DSC) result of SU-8 layer with and without platinum layer on top of it.

In most ALD processes, platinum film deposition involves surface combustion and dehydrogenation reactions with the use of (methylcyclopentadienyl)trimethylplatinum (MeCpPtMe3) and molecular oxygen (O_2) at elevated temperatures (> 200 °C).[1–4] Lower reaction temperatures may be realized through the use of plasma-excited species (e.g. H_2, O_2) or ozone (O_3)[5–8]. Films produced with these alternative counter-reactants are metallic Pt with minimal contamination, exhibit high electrical conductivity, and may be formed at lower temperatures, making their use ideal for Pt ALD on temperature-sensitive substrates such as polymers in our case. Using $MeCpPtMe_3$ and O3, we successfully deposited a Pt layer film on top of an SU-8 template at 200 °C.

After ALD process, a burning process in a convection oven at high temperature was selected to remove the SU-8 template under platinum layer completely. A differential scanning calorimetry

(DSC) test was performed for SU-8 layer on Si substrate with and without Pt layer on top of it to confirm a burning temperature, which usually at around 450 ~ 600 °C for efficient removal of SU-8.[9] As shown in Figure S1, the DSC result showed that there is a peak at around 500 °C for both cases, which indicates a melting point of SU-8 and Pt layer does not affect upon this thermal transition of polymer layer. Accordingly, a thermal process at 550 °C to remove polymer template was designed and a free-standing metallic Pt nano-accordion structure on Si substrate can be achieved.

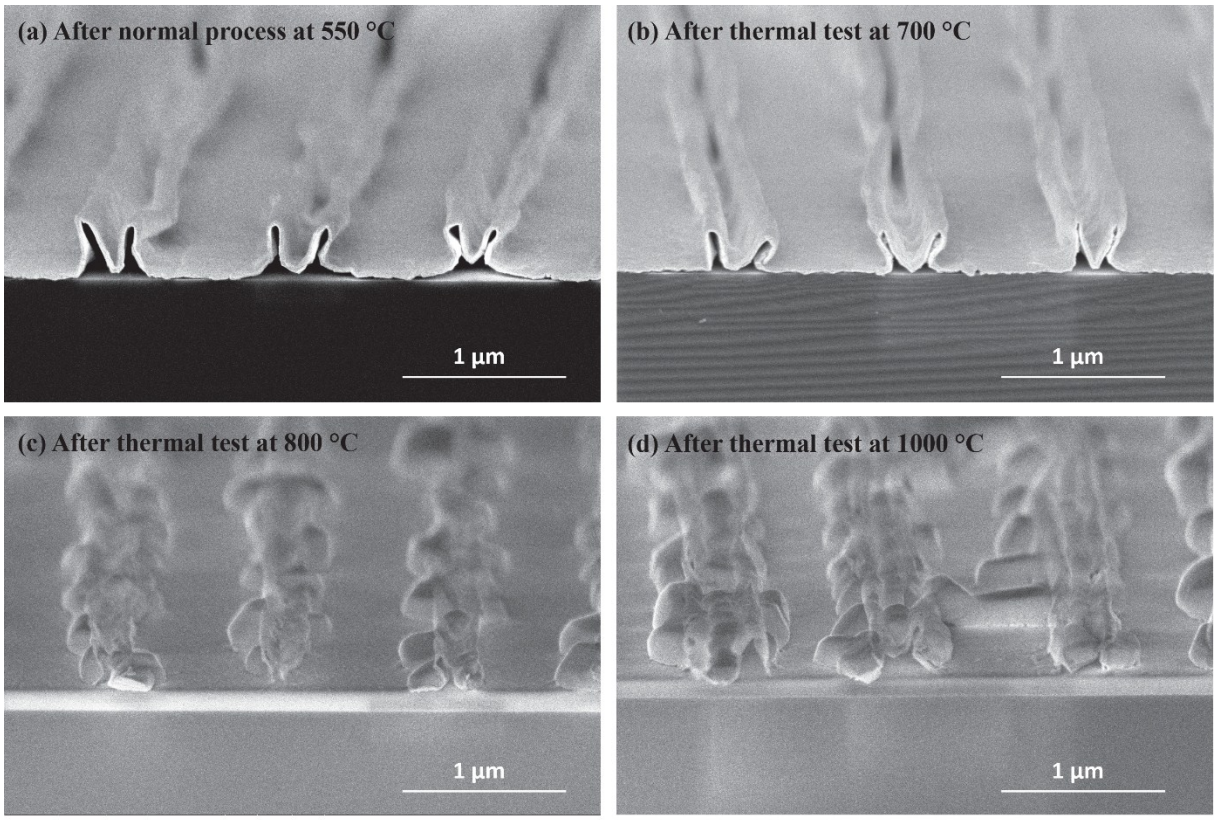

Figure S2. Cross-sectional view **S**EM images of Pt nano-accordions structures (DC = 60%, AR = 0.83) (a) after the normal temperature removal process at 550 °C, and after high temperature thermal tests at (b) 700 °C, (c) 800 °C, and (d) 1000 °C.

The thermal stability of platinum nano-accordion was examined by high temperature test using a convection oven. Until around 700 °C, the Pt nano-accordion remained its shape and electrical conductivity as before the thermal test, which is shown in Figure S2(a) and (b). However after 800 °C thermal test, the shape was deformed and a structural collapse occurred probably because of metal oxidation under high temperature[10] (Figure S2(c)). This dramatic change happened more extremely as temperature was increased to even higher temperature like 1000 °C, as in Figure S2(d), and the initial sprout-like profile was difficult to be distinguished from its cross-sectional view while the periodicity of the nano-accordion barely persisted.

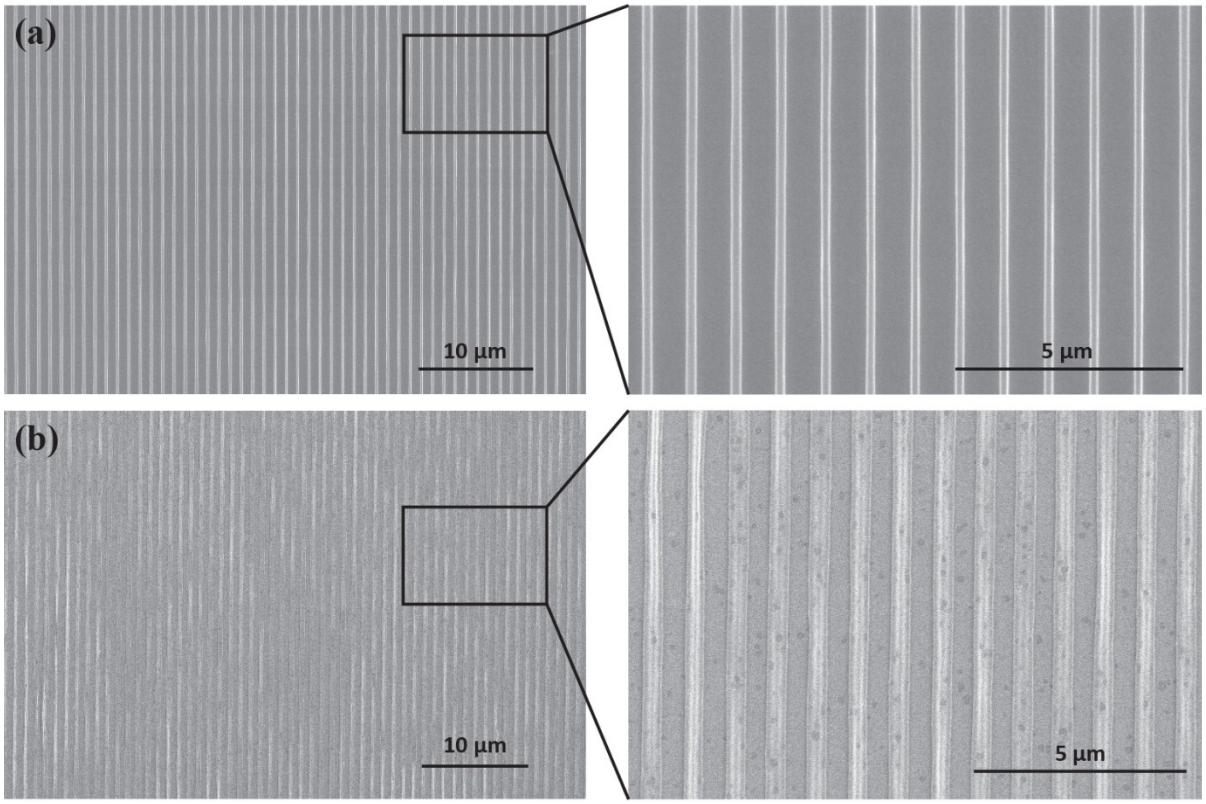

Figure S3. Top view SEM images of Pt nano-accordions structures with (a) wavy shape (DC = 50%, AR = 1.0) and (b) sprout-like shape (DC = 60%, AR = 0.83).

The structural stability of platinum nano-accordion after template removal process was confirmed by observing the overall quality of nanostructures in a large area under SEM. As shown in Figure S3, the Pt nanostructures showed an excellent quality through the whole sample area and the period of nano-accordion was kept as 1 μm even after thermal process.

Supplementary Information B: Effect of Intermediate Alumina Layer

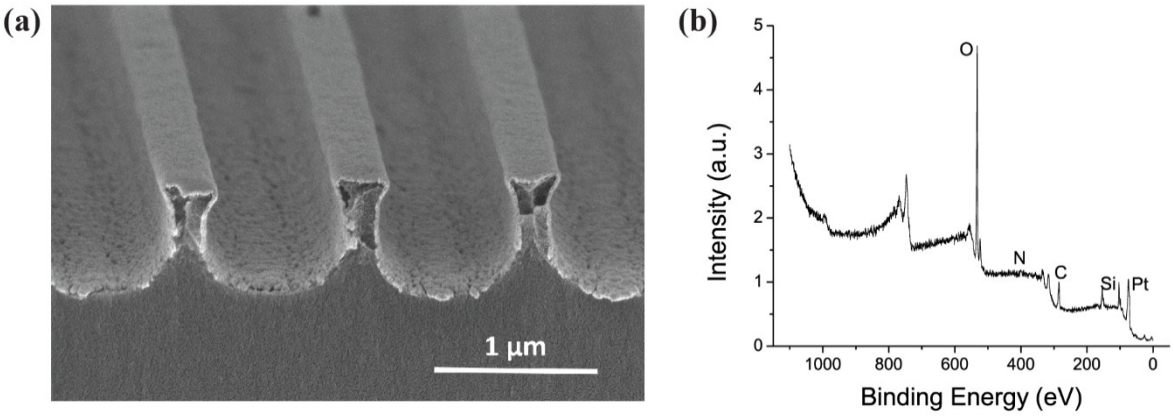

Figure S4. (a) SEM image of Pt Oxide film after direct Pt ALD coating on polymer template without intermediate layer of Al_2O_3 (b) XPS result for Pt Oxide film.

The first platinum ALD coating on polymer grating template was processed without employing intermediate Al_2O_3 layer. In these samples the Pt layers had relatively rough surface morphology, as seen in the SEM image of Figure S4(a). Such morphology was not observed when the same Pt ALD process was used on bare silicon and silicon oxide substrates. In addition, the thickness was less than 30 nm after 630 cycles of Pt ALD process, a reduction in the expected deposition rate of ~0.6-0.7 Å per ALD.[6–8] The structure profiles also changed dramatically because the platinum nuclei adhere poorly to the polymer template directly. The XPS measurements confirmed that the top layer is not pure Pt, since there is a weak peak for metallic Pt at 71.0 eV but a strong peak for oxygen components, indicating the presence of oxides (PtO_x) at 529 ~ 530 eV.[6] To avoid poor Pt deposition on polymer template, an intermediate layer of alumina was then introduced. This resulted in better Pt film morphology, electrical properties, and consistent thickness, as described in the main text.

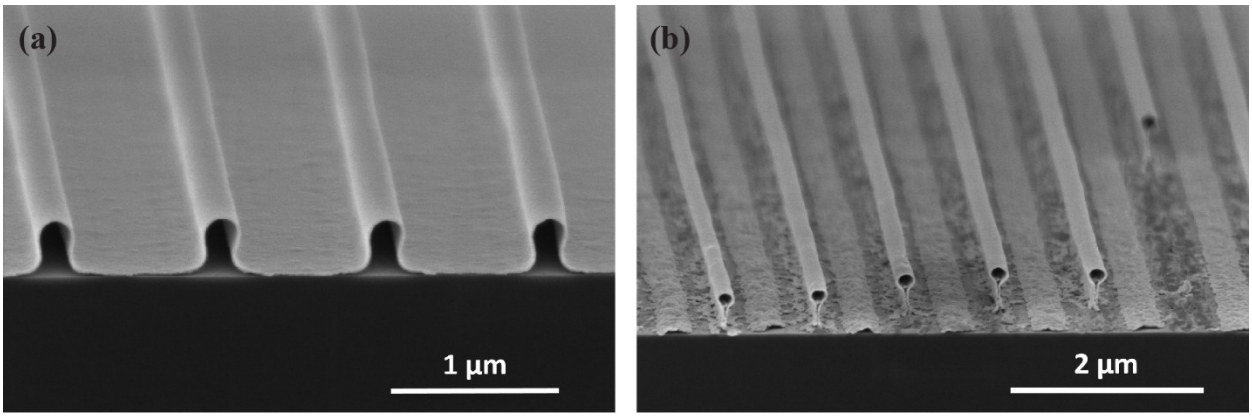

Figure S5. SEM images of platinum oxide nanostructures after template removal process; (a) Pt oxide nano-accordions (b) Pt oxide nano-pipe array.

While the Pt oxide samples can also yield similar nano-accordion structure, they resulted in poor structure fidelity after template removal. First, they are typically more flexible and forms a round-edged nano-accordion structures, as seen in Figure S5(a). For AR > 1, the two sidewalls collapse together and round ceiling result in a perfect circular profile, shown in Figure S5(b). However, the structure has significant film discontinuity due to cracking. Second, Pt oxide nano-accordions (t ~ 20 nm) have no reflective nature like a metal Pt layer and are mostly transparent. Also, their resistivity is significantly higher than Pt film and the calculated resistivity was around 10 Ω·cm, which obviously shows its non-metallic electrical property.[11]

Supplementary Information C: Electrical Property of Platinum Planar Film and Nano-Accordions before and after Template Removal

Sample Type	Thickness	Sheet Resistance (Ω/square)	Resistivity (μΩ·cm)
Planar Pt on SU-8	10 nm	19.50	19.50
Pt Nano-Accordion before Template Removal	20 nm	10.45 ($R_{\parallel}$)	20.90
		10.82 ($R_{\perp}$)	21.64
Pt Nano-Accordion after Template Removal	20 nm	10.34 ($R_{\parallel}$)	20.68
		10.86 ($R_{\perp}$)	21.72

Table S1. The sheet resistance and resistivity of platinum planar film and nano-accordions.

The sheet resistance and resistivity of platinum planar film and nano-accordions before and after template removal were measured and listed in Table S1. For the Pt nano-accordions, the period of polymer template was 1 μm, and the width and height of the grating were 500 nm, therefore the nano-accordions with a duty cycle of 50% and an aspect ratio of 1 were tested. For the planar film, no directional difference in electrical conductivity was observed. However for the nano-accordions, the sheet resistance in the perpendicular direction to the grating ($R_{\perp}$) was 3 ~ 5% higher than in the parallel direction ($R_{\parallel}$).

Supplementary Information D: Gradual Control of Aspect Ratio by Plasma Etching

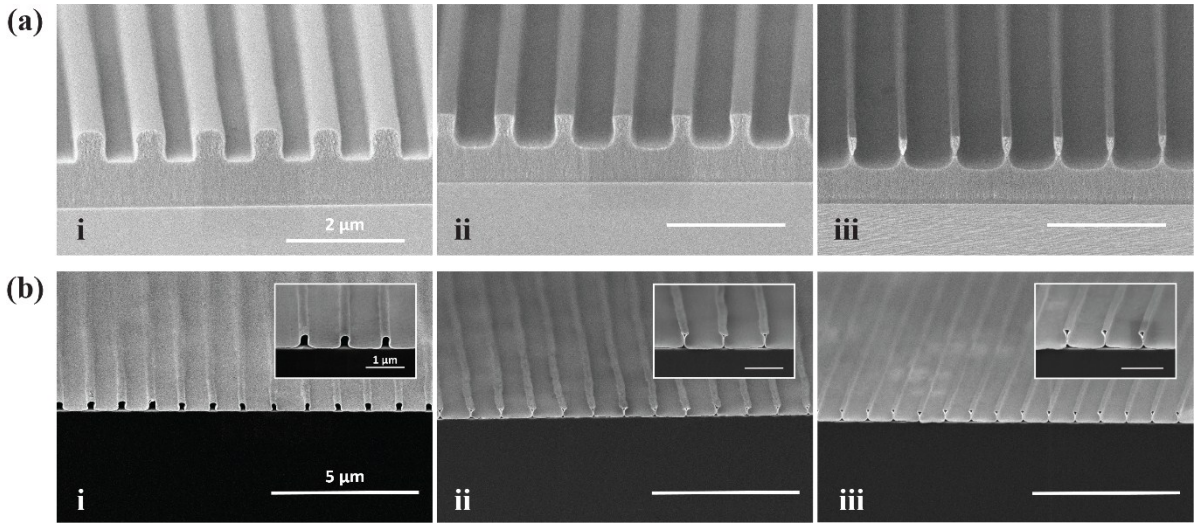

Figure S6. Aspect ratio of polymer grating template controlled by isotropic plasma etching. SEM images for each AR cases (a) before and (b) after template removal. Initial (i) AR = 1 sample was etched to obtain (ii) AR ~ 2 and (iii) AR ~ 5, with etch time of 3 min and 6 min, respectively.

As we demonstrated various profiles for round top cases, the AR of resist template can also be controlled with isotropic oxygen plasma etching. Figure S6 shows the gradual change of the polymer grating as the etching time is increased. Starting with AR = 1, the grating width can be shortened while the keeping height the same using 3 minutes of oxygen plasma etching (power of 300 W and pressure of 1 Torr). Further etching on polymer template have made a neck between grating layer and buffer layer, resulting in AR ~ 5. The upper side of neck formed a pipe profile and the lower side shaped a vertical column.

Supplementary Information E: Resistance Anisotropy vs. Aspect Ratio of Platinum Films and Nano-Accordions

Sheet Resistance (Ω/square)	Before Template Removal			After Template Removal		
	$R_{\parallel}$	$R_{\perp}$	Ratio ($R_{\perp}/R_{\parallel}$)	$R_{\parallel}$	$R_{\perp}$	Ratio ($R_{\perp}/R_{\parallel}$)
AR = 0.5	12.36±0.10	12.58±0.33	1.018	11.23±0.29	11.25±0.32	1.001
AR = 0.83	10.45±0.19	10.82±0.37	1.036	10.25±0.16	11.25±0.38	1.098
AR = 1.33	12.62±0.26	13.46±1.33	1.066	11.37±0.15	14.39±0.24	1.265
AR = 1.71	11.39±0.32	12.30±0.27	1.081	13.79±0.51	17.76±0.39	1.288
AR = 2.0	11.92±1.04	13.17±0.84	1.105	12.57±0.34	18.31±0.42	1.456

Table S2. Sheet resistance and anisotropy ratio of platinum films and nano-accordions before and after template removal for 5 different AR cases.

The directional difference of sheet resistance of Pt nano-accordions before and after template removal was further studied with different aspect ratios and structure profiles. We prepared 5 different AR samples varying with different polymer thickness and different oxygen plasma etching time, where AR = 0.5, 0.83, 1.33, 1.71 and 2, as shown in Table S2. When AR = 0.5, the sheet resistance remained about the same in either directions parallel or perpendicular to the structure ridge direction, and the template removal process did not have an effect. When AR = 0.83, the anisotropy ratio increased to 3.6% and 9.8% for before and after template removal, respectively, which reflected the increased surface roughness by sharper edges and cracks of the structure.[12] For the most extreme case with AR = 2, the anisotropy was more dramatic. The measured data indicate that the perpendicular resistance is 10% and 45% higher than the parallel resistance for before and after template removal, respectively. Compared to the free-standing samples, the effect of AR before template removal is less significant over the anisotropy. Figure 7 represents the measuring results on anisotropic resistance ratio depending on the polymer template's aspect ratio.

References

1 T. Aaltonen, M. Ritala, T. Sajavaara, J. Keinonen and M. Leskelä, *Chem. Mater.*, 2003, **15**, 1924–1928.

2 T. Aaltonen, M. Ritala, Y.-L. Tung, Y. Chi, K. Arstila, K. Meinander and M. Leskelä, *J. Mater. Res.*, 2004, **19**, 3353–3358.

3 A. J. M. MacKus, N. Leick, L. Baker and W. M. M. Kessels, *Chem. Mater.*, 2012, **24**, 1752–1761.

4 I. J. M. Erkens, A. J. M. Mackus, H. C. M. Knoops, P. Smits, T. H. M. van de Ven, F. Roozeboom and W. M. M. Kessels, *ECS J. Solid State Sci. Technol.*, 2012, **1**, P255–P262.

5 A. J. M. MacKus, D. Garcia-Alonso, H. C. M. Knoops, A. a. Bol and W. M. M. Kessels, *Chem. Mater.*, 2013, **25**, 1769–1774.

6 J. Dendooven, R. K. Ramachandran, K. Devloo-Casier, G. Rampelberg, M. Filez, H. Poelman, G. B. Marin, E. Fonda and C. Detavernier, *J. Phys. Chem. C*, 2013, **117**, 20557–20561.

7 H. B. R. Lee, K. L. Pickrahn and S. F. Bent, *J. Phys. Chem. C*, 2014, **118**, 12325–12332.

8 J. Z. Mundy, A. Shafiefarhood, F. Li, S. A. Khan and G. N. Parsons, *J. Vac. Sci. Technol. A Vacuum, Surfaces, Film.*, 2016, **34**, 01A152.

9 P. M. Dentinger, W. M. Clift and S. H. Goods, *Microelectron. Eng.*, 2002, **61-62**, 993–1000.

10 A. R. Powell, *Platin. Met. Rev.*, 1958, **2**, 95–98.

11 J. Hämäläinen, F. Munnik, M. Ritala and M. Leskelä, *Chem. Mater.*, 2008, **20**, 6840–6846.

12 H. Marom and M. Eizenberg, *J. Appl. Phys.*, 2006, **99**, 1–8.